# Large bandwidth mode order converter by differential waveguides

**Article** *in* Optics Express · February 2015

DOI: 10.1364/OE.23.003186

CITATIONS
6

READS
47

**5 authors**, including:

Bilgehan Barış Öner
TOBB University of Economics and Technology
**20** PUBLICATIONS **73** CITATIONS
SEE PROFILE

Hamza Kurt
TOBB University of Economics and Technology
**159** PUBLICATIONS **1,199** CITATIONS
SEE PROFILE

Ali K. Okyay
Bilkent University
**169** PUBLICATIONS **1,839** CITATIONS
SEE PROFILE

Gonul Turhan-Sayan
Middle East Technical University
**81** PUBLICATIONS **690** CITATIONS
SEE PROFILE

# Large bandwidth mode order converter by differential waveguides

**B. B. Oner,[1,5,*] K. Üstün,[2,3,5] H. Kurt,[1] A. K. Okyay,[4] and G. Turhan-Sayan[2]**

[1] *Nanophotonics Research Laboratory, Department of Electrical and Electronics Engineering, TOBB University of Economics and Technology, 06560 Ankara, Turkey*
[2] *Department of Electrical and Electronics Engineering, Middle East Technical University, 06800 Ankara, Turkey*
[3] *Department of Electrical and Electronics Engineering, Hitit University, 19030 Çorum, Turkey*
[4] *Department of Electrical and Electronics Engineering, UNAM-National Nanotechnology Research Center, Institute of Materials Science and Nanotechnology, Bilkent University, 06800, Turkey*
[5] *These authors contributed equally to this work.*
[*] *bilgehan.oner@gmail.com*

**Abstract:** In this article, we propose a large bandwidth mode-order converter design by dielectric waveguides with equal lengths but different cross-sectional areas. The efficient conversion between even and odd modes is verified by inducing required phase difference between the equal length waveguides of different widths. Y-junctions are composed of both tapered mode splitter and combiner to connect mono-mode waveguide to multi-mode waveguide. The converted mode profiles at the output port show that the device operates successfully at designed wavelengths with wide bandwidth. This study provides a novel technique to implement compact mode order converters and direction selective/sensitive photonic structures.



**OCIS codes:** (130.2790) Guided waves; (230.7370) Waveguides; (130.3120) Integrated optics devices.

## References and links

1. A. C. Ruege and R. M. Reano, "Multimode waveguide-cavity sensor based on fringe visibility detection," Opt. Express **17**(6), 4295–4305 (2009).
2. V. Liu, D. A. Miller, and S. Fan, "Ultra-compact photonic crystal waveguide spatial mode converter and its connection to the optical diode effect," Opt. Express **20**(27), 28388–28397 (2012).
3. V. R. Almeida, C. A. Barrios, R. R. Panepucci, and M. Lipson, "All-optical control of light on a silicon chip," Nature **431**(7012), 1081–1084 (2004).
4. H. Kurt, B. B. Oner, M. Turduev, and I. H. Giden, "Modified Maxwell fish-eye approach for efficient coupler design by graded photonic crystals," Opt. Express **20**(20), 22018–22033 (2012).
5. T. Shoji, T. Tsuchizawa, T. Watanabe, K. Yamada, and H. Morita, "Low loss mode size converter from 0.3 μm square Si wire waveguides to singlemode fibres," Electron. Lett. **38**(25), 1669–1670 (2002).
6. R. C. Alferness and L. L. Buhl, "Electro-optic waveguide TE TM mode converter with low drive voltage," Opt. Lett. **5**(11), 473–475 (1980).
7. Y. Huang, G. Xu, and S.-T. Ho, "An ultracompact optical mode order converter," Photon. Technol. Lett. **18**(21), 2281–2283 (2006).
8. M. W. Pruessner, J. B. Khurgin, T. H. Stievater, W. S. Rabinovich, R. Bass, J. B. Boos, and V. J. Urick, "Demonstration of a mode-conversion cavity add-drop filter," Opt. Lett. **36**(12), 2230–2232 (2011).
9. J. Castro, D. F. Geraghty, S. Honkanen, C. M. Greiner, D. Iazikov, and T. W. Mossberg, "Demonstration of mode conversion using anti-symmetric waveguide Bragg gratings," Opt. Express **13**(11), 4180–4184 (2005).
10. J. E. Castillo, J. M. Castro, R. K. Kostuk, and D. F. Geraghty, "Study of multichannel parallel anti-symmetric waveguide Bragg gratings for telecom applications," Photon. Technol. Lett. **19**(2), 85–87 (2007).
11. B. B. Oner, M. Turduev, I. H. Giden, and H. Kurt, "Efficient mode converter design using asymmetric graded index photonic structures," Opt. Lett. **38**(2), 220–222 (2013).
12. M. Turduev, B. Oner, I. Giden, and H. Kurt, "Mode transformation using graded photonic crystals with axial asymmetry," J. Opt. Soc. Am. B **30**(6), 1569–1579 (2013).
13. J. R. Kurz, J. Huang, X. Xie, T. Saida, and M. M. Fejer, "Mode multiplexing in optical frequency mixers," Opt. Lett. **29**(6), 551–553 (2004).
14. N. Erim, I. Giden, M. Turduev, and H. Kurt, "Efficient mode-order conversion using a photonic crystal structure with low symmetry," J. Opt. Soc. Am. B **30**(11), 3086–3094 (2013).

#226827 - $15.00 USD Received 13 Nov 2014; revised 12 Jan 2015; accepted 16 Jan 2015; published 3 Feb 2015

15. Y. B. Cho, B. K. Yang, J. H. Lee, J. B. Yoon, and S. Y. Shin, "Silicon photonic wire filter using asymmetric sidewall long-period waveguide grating in a two-mode waveguide," Photon. Technol. Lett. **20**(7), 520–522 (2008).
16. P. Qu, C. Liu, W. Dong, W. Chen, F. Li, H. Li, Z. Gong, S. Ruan, X. Zhang, and J. Zhou, "Design of a vector-sum integrated microwave photonic phase shifter in silicon-on-insulator waveguides," Appl. Opt. **50**(17), 2523–2530 (2011).
17. L. H. Frandsen, Y. Elesin, L. F. Frellsen, M. Mitrovic, Y. Ding, O. Sigmund, and K. Yvind, "Topology optimized mode conversion in a photonic crystal waveguide fabricated in silicon-on-insulator material," Opt. Express **22**(7), 8525–8532 (2014).
18. J. Feng, Y. Chen, J. Blair, H. Kurt, R. Hao, D. S. Citrin, C. J. Summers, and Z. Zhou, "Fabrication of annular photonic crystals by atomic layer deposition and sacrificial etching," J. Vac. Sci. Technol. B **27**(2), 568–572 (2009).
19. N. Riesen and J. D. Love, "Design of mode-sorting asymmetric Y-junctions," Appl. Opt. **51**(15), 2778–2783 (2012).
20. S. G. Leon-Saval, A. Argyros, and J. Bland-Hawthorn, "Photonic lanterns: a study of light propagation in multimode to single-mode converters," Opt. Express **18**(8), 8430–8439 (2010).
21. D. Dai, J. Wang, and Y. Shi, "Silicon mode (de)multiplexer enabling high capacity photonic networks-on-chip with a single-wavelength-carrier light," Opt. Lett. **38**(9), 1422–1424 (2013).
22. N. Riesen and J. D. Love, "Tapered Velocity Mode-Selective Couplers," J. Lightwave Technol. **31**(13), 2163–2169 (2013).
23. D. Dai, Y. Tang, and J. E. Bowers, "Mode conversion in tapered submicron silicon ridge optical waveguides," Opt. Express **20**(12), 13425–13439 (2012).
24. D. Ohana and U. Levy, "Mode conversion based on dielectric metamaterial in silicon," Opt. Express **22**(22), 27617–27631 (2014).
25. S. Johnson and J. Joannopoulos, "Block-iterative frequency-domain methods for Maxwell's equations in a planewave basis," Opt. Express **8**(3), 173–190 (2001).
26. A. F. Oskooi, D. Roundy, M. Ibanescu, P. Bermel, J. D. Joannopoulos, and S. G. Johnson, "MEEP: a flexible free-software package for electromagnetic simulations by the FDTD method," Comput. Phys. Commun. **181**(3), 687–702 (2010).
27. A. Taflove and S. C. Hagness, *Computational Electrodynamics: The Finite-Difference Time-Domain Method* (Artech House, 2005).
28. J. P. Berenger, "A perfectly matched layer for the absorption of electromagnetic waves," J. Comput. Phys. **114**(2), 185–200 (1994).

## 1. Introduction

In recent decades, along with the rapid development and diversity of photonic structures, the demand for mode conversion process has received a considerable interest. Cavity biosensors [1], direction selective structures [2], and all-optical switching [3] are some of the applications that mode conversion concept is utilized. The term mode conversion has different meanings according to the change that the mode undergoes. One of the conversion schemes deals with the manipulation of the optical mode size [4, 5]. Another method addresses polarization conversion of waveguide modes, i.e., TE-TM mode conversion [6]. Finally, some converter designs include transforming one optical mode to the other with different mode order. Such a conversion is also a preliminary method to acquire one-way (unidirectional) propagation of light. Placing an even-odd mode converter between single and multimode waveguides causes an even input mode to propagate in only one way. Namely, the input fundamental mode at one side is transmitted to the other side but the fundamental mode of the output waveguide is not transmitted in the backward direction.

There have been several methods in order to achieve mode order conversion [2, 7–17]. One of these methods is based on Bragg gratings which have high reflection/transmission efficiency but require long distances to achieve conversion [9, 10]. Another method is mode order transformation by two-dimensional graded index photonic crystals [11, 12]. Similarly, a recent approach utilized modified annular photonic crystals [18] that provide remarkably high bandwidth but relatively lower transmission efficiency due to input and output coupling losses [14]. In Ref. 2, authors suggested that an optimization process for a region in photonic crystal waveguide provides a compact mode order converter. However, also this optimization method did not achieve large operating bandwidth. Mode conversion process can also be realized in different ways such as asymmetric Y-junctions, photonic lanterns, directional

#226827 - $15.00 USD Received 13 Nov 2014; revised 12 Jan 2015; accepted 16 Jan 2015; published 3 Feb 2015

couplers, and lateral tapers [19–23]. Mode multiplexers / demultiplexers utilize the conversion with relatively short coupling lengths with a limited bandwidth [21]. Mode selective couplers present low wavelength dependency while they require really large footprint [22]. In Ref. 23, both mode order and orthogonal polarization conversions are achieved. Similarly, the disadvantage of this approach is the need of remarkably long taper lengths to obtain an efficient conversion. One of the recent works achieves mode conversion by using dielectric meta-material in silicon [24]. Refractive index variation of dielectric waveguide is calculated to enable conversion with high efficiency between different mode orders. Besides, effective medium theory is utilized to generate more practical designs. Main concept of our approach is different from the previous studies and also provides an arrangement to the trade-off between bandwidth and conversion length. We propose a mode-order converter design performing a conversion between the fundamental (even) and second order (odd) modes with a simpler geometry that can be fabricated more easily than the approaches utilizing photonic crystals. The mode order conversion is based on two differential dielectric waveguides. Different width ($w$) values of the waveguides give rise to different effective wave vectors (and consequently different phase accumulations during light propagation). Two waveguides that differ in width could be used in order to introduce a phase difference between the two equal power beams propagating in Y branches. Namely, for a specified length, a phase difference of $\Delta\Phi = \pi$ can be imposed at a selected frequency.

To summarize the rest of the paper, the methodology of the mode converter design is elaborated with both frequency and time domain analyses in the next section. In Section 3, findings of the study are discussed along with a brief comparison with the literature. Finally, conclusions are presented in Section 4.

## 2. Numerical analyses and design methodology

### *2.1 The frequency domain analysis*

The main aim of the study is to achieve a simple mode order converter operating in a large bandwidth. Therefore, frequency domain numerical analysis is first performed to reveal dispersion characteristic of the rectangular Silicon waveguides, on a silica ($n_{SiO2}$ = 1.5) substrate. The schematic view of the proposed structure is given in Fig. 1(a). The details of the structural parameters are shared later in the text. Three dimensional (3D) plane wave expansion method is employed [25]. Width ($w$) and thickness ($t$) parameters of the waveguide are key parameters affecting the wave vector magnitude which is a function of operating frequency. In our analyses, we keep $t$ constant because adjusting the thickness of the waveguides may become more difficult compared to the width value during the fabrication stage. Hence, we only varied $w$ to obtain distinct waveguides.

Transverse electric-like polarization type is considered in the study. For maximizing the bandwidth, dispersion diagrams (relation between normalized frequency and normalized propagation vector) of rectangular waveguides ($n_{Si}$ = 3.46) with different widths are computed. Afterwards, the data that gives the phase difference of the two arms per length, is calculated as $\Delta\Phi = L\Delta k$, where $\Delta k = |k_1\text{-}k_2|$ is the wave vector difference between the two waveguides. . It is noticed that difference between the propagation vectors ($\Delta k$) stays almost constant for a spectral region as shown in Fig. 1(b) (shaded region). In this manner, one can infer that the propagating light waves in these waveguides are exposed to almost the same phase difference within this frequency region. For a determined frequency, a conversion length ($L_c$) can be calculated for $\pi$ (180°) phase shift with the known $\Delta k$ value, $L_c = \pi/\Delta k$. One of the most important points is determining the reference length providing the largest operating bandwidth.

Firstly, in our approach, we assumed 5° phase shift error as negligible and calculated upper and lower frequency limits in order to obtain a starting point for the time domain analysis. Assuming 5° phase error to be acceptable enables us to carry out the analysis. One

#226827 - $15.00 USD Received 13 Nov 2014; revised 12 Jan 2015; accepted 16 Jan 2015; published 3 Feb 2015

may question the validity of this selection rule. Relatively larger phase error estimations will result inefficient performance comparisons because the efficiency of conversion is related with the cosine of the phase error. The difference between cosine values of no phase error (0°) and 5° is less than 0.005 that would hardly reduce the conversion performance. A basic method could be choosing a normalized frequency that corresponds to the peak point as the center and the frequencies that cause 5° error as the upper and lower frequency limits. However, we have chosen the error of 5° for the peak of $\Delta k$ spectrum and we determined both the upper and lower limit of frequency interval admitting −5° error at these frequencies, and the estimated bandwidth is determined accordingly as an apriori assumption for time domain analysis. In this way the upper and lower limits of the frequency region are extended.

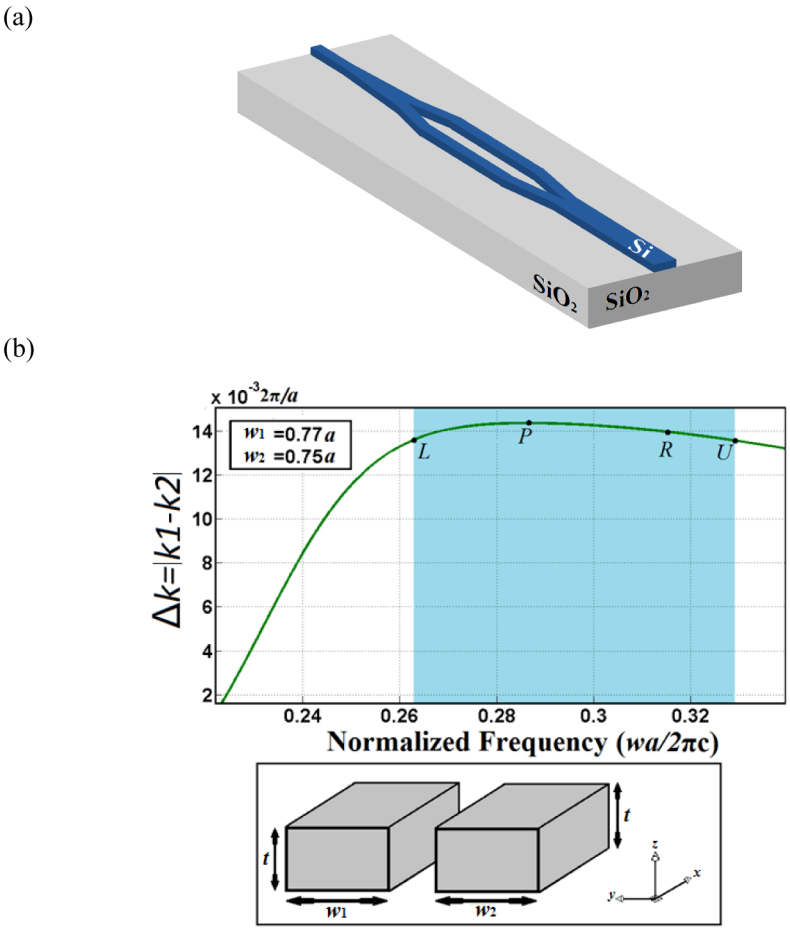


Fig. 1. (a) 3D schematic view of the designed mode order converter device. (b) Frequency dependence of the difference between propagation wave-vectors ($\Delta k$). Almost negligible frequency dependency at the proximity of the peak point enables large bandwidth conversion. The symbol $R$ represents the reference point that the waveguide length is determined accordingly. The phase shift error between the peak point ($P$) and $R$ is 5°. Phase shift error between $R$ and the upper limit ($U$) equals to the error between $R$ and the lower limit ($L$) that is also 5°.

Maximizing the bandwidth with this method by choosing arbitrarily small width difference between the two waveguides is theoretically possible; however, this would cause a substantial increase in the conversion length, $L_c$. In other words, there is a trade-off between bandwidth and the conversion length. To have a compact design, bandwidth can be

#226827 - $15.00 USD Received 13 Nov 2014; revised 12 Jan 2015; accepted 16 Jan 2015; published 3 Feb 2015

compromised. The relation between bandwidth and size of the device is given in detail in later in this paper. Considering this relation, the optimized waveguide width difference is determined as $0.02a$ and the waveguide widths are chosen as $w_1 = 0.77a$ and $w_2 = 0.75a$ with the thickness $t_1 = t_2 = 0.70a$, where $a$ is the scaling length constant. Lastly, the optimized $\Delta k$ and conversion length values are calculated as $\Delta k = 2\pi \times 0.013977a^{-1}$ and $L_c = 35.77a$, respectively.

*2.2 The time domain analysis*

The required structural parameters presented in the previous section are calculated in the frequency domain analyses. Three dimensional finite-difference time-domain (FDTD) analyses are also carried out in order to demonstrate the efficiency of the mode order conversion process, present one-way propagation characteristic with transmission efficiencies and the π phase shift with the differential waveguides [26, 27]. The computational window is surrounded by perfectly matched layers to avoid reflections occurring at the boundaries [28]. In time domain computations, a grid size of $\Delta x = \Delta y = a/30$ is implemented.

In order to fully accomplish the mode order conversion operation, a complete design is necessary which consists of power divider, phase shifter and power combiner. Y-junctions are needed to separate the input beam into two equal parts and to combine the π phase shifted beams. The input and the output waveguides with different sizes (for different mode-supporting characteristics) are needed to achieve one way propagation. Finally, differential waveguides that are analyzed in the previous section are required to achieve the π phase shift. The geometry of the full design is given in Fig. 2. While Fig. 2(a) demonstrates the top view of structure presented in Fig. 1(a), the lower section, Fig. 2(b) designates values of the all parameters in detail.

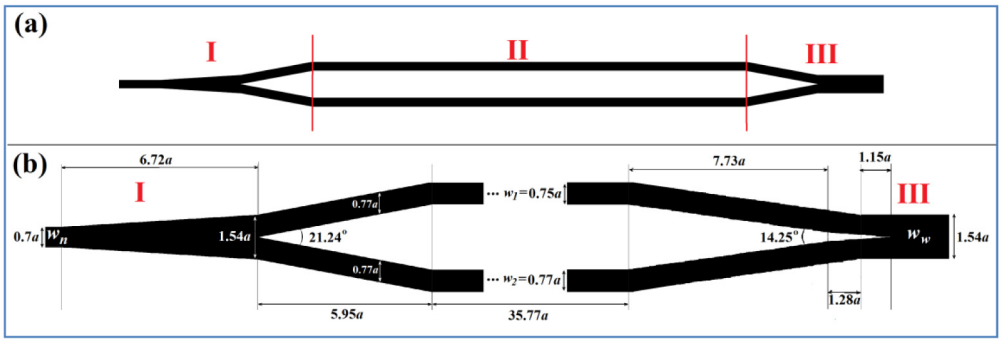


Fig. 2. (a) The top view of the converter design. Part I and III enables splitting and combining of the propagating beams. Phase shifting occurs in Part II. (b) Zoom-in views of the Part I and III are given with structural parameters in detail.

Transmission spectrum of the structure is computed via time domain simulations. In this manner, contrast ratio is defined as $(T_f\text{-}T_b)/(T_f + T_b)$ and calculated between the two transmission spectra of the structure with different directions, where $T_f$ and $T_b$ correspond to forward and backward transmission values, respectively. This calculation shows an indirect figure of merit for the mode order conversion effectiveness. The narrow waveguide port $w_n$ only supports the even mode, and the wide waveguide port $w_w$ supports both even and odd modes. It is expected that high transmission characteristic should be observed within the operating frequency interval if the beam propagates from $w_n$ to $w_w$ (forward propagation from even mode to odd mode). Moreover, almost perfect reflection and/or leakage from waveguide to environment of even mode is expected if the propagation direction is inverted (backward propagation) due to the mode supporting features of the waveguides mentioned above. However, this reflected beam is not desirable because it may be guided back to the input

#226827 - $15.00 USD Received 13 Nov 2014; revised 12 Jan 2015; accepted 16 Jan 2015; published 3 Feb 2015

waveguide port and this would harm the operation of the components at the output side. Another cause of problem is unwanted losses through the junctions that can degrade transmission in forward direction. In order to overcome all these issues, the angle between each Y-junction branch is carefully selected and tapered transitions are added to both sides to obtain optimum contrast ratio and have minimum reflection. Consequently, escaping of the unwanted mode from the waveguide as radiation is promoted. This is accomplished by a tapered waveguide that matches a multimode waveguide to a single mode one. Hence, higher order modes cannot survive in the structure but couple to radiation modes. In the other case where there is no tapering region, the junction will reflect a significant portion of optical wave, and this may re-couple to the excitation side, producing all of the drawbacks as explained above.

We may propose the methodology as a kind of wave vector matching problem. Therefore, a simple Y-junction is, in principle adequate. However, structural parameters of the junctions have effect on performance of the converter, for instance, transmission efficiency and contrast ratio. The design parameters are achieved for aiming to increase the forward transmission above 90%. Each variable is sequentially updated and transmission efficiency is monitored. The angle value is scanned in the radian units, hence there is a fraction when it is converted into the degree units. The top view of the overall design given in Fig. 1(a) is shown in Fig. 2. The detailed schematics of the junctions with structural parameters for parts I and III are given in Fig. 2(b).

Figure 3(a) depicts transmission efficiency of the structure for the forward and backward propagations. These efficiencies are calculated under the case that fundamental mode acts as an excitation source for the two cases (higher orders are not supported at the input side as mentioned above). Backward transmission efficiency should be also used to compute mode order conversion efficiency. A perfect conversion provides zero transmission in backward direction which is equivalent to perfect mode order conversion efficiency as the

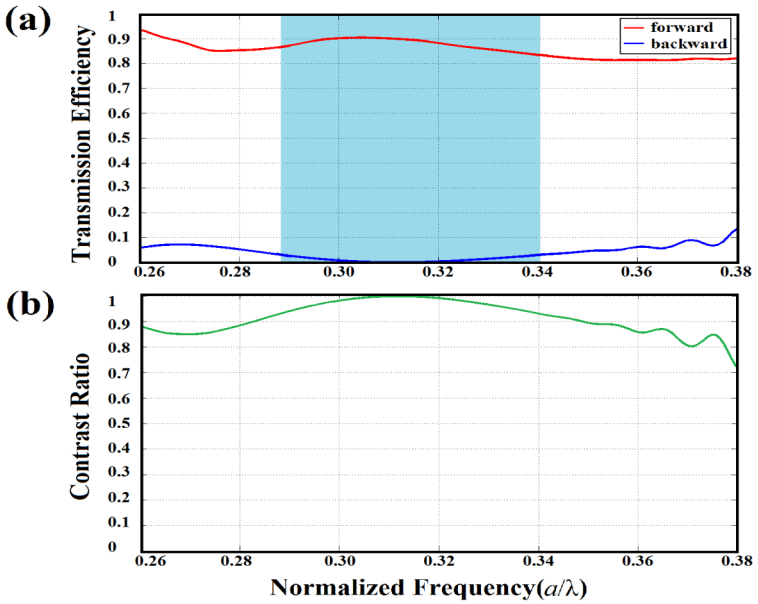


Fig. 3. (a) Forward and backward transmission efficiencies are given. The shaded region represents the operating frequency regime. (b) Contrast ratio of the design with the given efficiencies is plotted.

#226827 - $15.00 USD Received 13 Nov 2014; revised 12 Jan 2015; accepted 16 Jan 2015; published 3 Feb 2015

narrow input waveguide (with the thickness $w_n$) supports only fundamental even mode. This is achieved only for a single frequency as mentioned in the Section 2.1. Therefore while calculating the bandwidth a tolerance factor $J$ can be defined as [2]:

$$J = \int_{\omega_{\min}}^{\omega_{\max}} \frac{(1-p_\omega)^2}{(\omega_{\max}-\omega_{\min})} d\omega \ , \tag{1}$$

where $\omega_{\min}$ and $\omega_{\max}$ are chosen minimum and maximum normalized operating frequencies and $p_\omega$ is conversion efficiency. If the operating limit of the maximum backward transmission efficiency is taken as 5% then, according to Eq. (1), this leads to a negligible tolerance $J < 6.7 \times 10^{-4}$ within 24% bandwidth. The bandwidth is defined as $(f_{max}\text{-}f_{min})/f_{cen}$, where $f_{min}$ and $f_{max}$ are the minimum and maximum frequency values, respectively. They satisfy the desired optimum efficiency value and $f_{cen}$ is the center frequency $(f_{max} + f_{min})/2$. The bandwidth becomes 16% if the transmission is assumed to be below 3%. The interval is shaded in Fig. 3(a). In the same frequency regions, forward transmission stays between 80% and 90%. It would be possible to achieve 100% transmission if the only concern was the phase error. The other problem to consider is the mode shape mismatch between the fundamental and higher order modes. This can be analyzed by the orthogonality relations and $k$-vector space decompositions, which is outside of the scope of the current study. Furthermore, high transmission efficiency of the forward propagation enables high contrast ratio which is given in Fig. 3(b). Hence, the criteria for the bandwidth calculation can also be determined according to the contrast ratio. Bandwidths of 30% and 20% are achieved, where the criteria is achieving contrast ratios over 85% and 90% respectively.

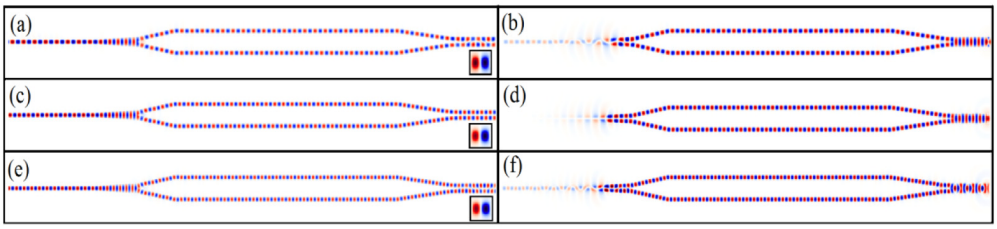


Fig. 4. Single frequency time domain snapshots for different operating frequencies are given. Lower frequency (a) forward, (b) backward propagation. Optimum frequency (c) forward, (d) backward propagation. Upper frequency (e) forward, (f) backward propagation. Electric field profiles along the out-of-plane are also given as insets for backward propagation cases.

In Fig. 4, steady state electric field snapshots of FDTD simulations are shown. All time-domain simulations are performed with continuous source excitation at a single frequency. The lower and upper frequencies ($a/\lambda = 0.2887$ and $a/\lambda = 0.3401$, respectively) are determined based on the backward propagation where the transmission efficiency falls down to 3%. An additional simulation is carried out for the optimum frequency $a/\lambda = 0.3117$ where the backward transmission has its minimum value (almost zero). Optimum frequency performs the best result as compared to lower and upper frequency values for the backward propagation conditions as can be seen in Fig. 4. An important point is the computed normalized frequency differences between the time domain and frequency domain analyses. The optimum frequency value is expected to correspond $R$ in Fig. 1(b). These two methods use distinctly different approaches for solving the electromagnetic field equations. The difference between normalized reference frequencies is $\Delta(a/\lambda) = 0.003$ which can be accepted as a negligible deviation.

The fundamental mode transforms into one higher mode for forward propagation case with high efficiency as shown in Figs. 4(a), 4(c) and 4(e), due to the fact that there is no large structural disturbance that can reflect the light. In addition, small angle at the Y-junctions

#226827 - $15.00 USD Received 13 Nov 2014; revised 12 Jan 2015; accepted 16 Jan 2015; published 3 Feb 2015

positively contributes the forward propagation efficiency. For the backward propagation case, the waveguide width, $w_n$, cannot support the confinement of the converted odd mode. Leakage of the optical wave to sides is observed at the junction by the help of the tapered region between junction and the waveguide. Thus, the transmission efficiency dramatically falls almost to zero for the backward propagation cases as demonstrated in Figs. 4(b), 4(d) and 4(f).

## 3. Discussion

In this work, we propose a novel method for mode order conversion with differential rectangular waveguides. In order to turn the design into a practical device, the structural parameters should be converted to metric system. If the center wavelength $\lambda = 3.2082a$ is chosen to correspond C-band at around 1550 nm, then the scaling parameter $a$ and conversion length, where $\pi$ phase shift occurs, should be around 483 nm and 17.28 μm, respectively. Accordingly, the waveguide widths are approximately $w_n = 338$ nm, $w_w = 744$ nm, $w_1 = 372$ nm and $w_2 = 362$ nm, where the thickness is $t = 338$ nm. Total dimensions of the design in the lateral and transverse directions are approximately 25.34 μm and 1.82 μm, respectively. These aspects of the geometry are feasible with the current micro-fabrication technologies. The lower and upper limit of operation wavelengths are around 1.42 μm and 1.67 μm, respectively.

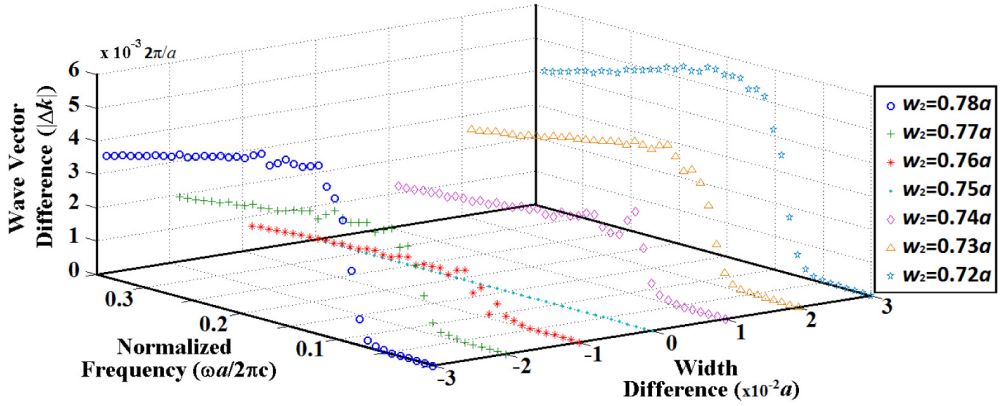


Fig. 5. Frequency and width difference ($\Delta w = w_1 - w_2$) dependency of $\Delta k$ is plotted. One of the waveguide thickness is fixed at $w_1 = 0.75a$ for varying values of $w_2 = [0.72a\text{-}0.78a]$.

Structural parameters are determined with respect to the method given in Section 2. As mentioned in the same section, this method enables increasing the operating bandwidth while decreasing the waveguide width difference ($\Delta w$). In other words, the operating frequency interval, where $\Delta k$ is assumed to stay constant, depends on $\Delta w$. This relation is shown in Fig. 5 which is plotted by keeping one of the waveguide widths constant and varying the other one. Choosing $\Delta w = 0$ makes the propagation vector difference zero as well for the entire frequency region, which corresponds to infinite length for conversion. As $\Delta w$ is increased, operating frequency interval gets narrower and conversion length gets smaller. The structural parameters $w_1$ and $w_2$ are determined considering the size of the device and current fabrication technologies. The dispersion curves of the corresponding waveguides are given in Fig. 6. The three normalized frequencies of 0.2887, 0.3117 and 0.3401 are also shown in the corresponding diagrams. As we can see in Fig. 6(a), when the width of the waveguide slightly increases, dispersion curves experience shift to lower frequencies and waveguide supports only single mode. On the other hand, when waveguide width becomes $1.54a$ as in Fig. 6(b), two bands corresponding fundamental even and higher order odd modes appear in the dispersion diagram.

#226827 - $15.00 USD Received 13 Nov 2014; revised 12 Jan 2015; accepted 16 Jan 2015; published 3 Feb 2015

The converter structures with Bragg gratings have high transmission/reflection efficiency but they lack in terms of bandwidth and compactness [9, 10]. There are more compact studies in the literature [2, 11, 12]. Ref. 2 investigated 2D photonic crystal structure without considering out-of plane losses and input/output coupling problems. Besides, the design utilizes resonant type structure that is inherently narrowband. However the proposed design is advantageous over previous ones with respect to transmission efficiency, bandwidth, and feasibility in the implementation. We should summarize brief comparison between current study and Ref. 7 as follows. In Ref. 7, mode order conversion is achieved with asymmetric junction branches. Even though the phase delay mechanism is similar with the current study, in our approach operating frequency regime is enhanced with a different implementation. Inequality of the parallel waveguides leading the phase delay is obtained by different waveguide widths but same propagating length values are taken. Therefore, this study provides a novel and feasible mode order conversion with one-way propagation. We should also note that the designed structure does not violate the reciprocity. If the converted odd mode in Figs. 4(a), 4(c) and 4(e) are used as input sources for the backward illumination cases, similar reciprocal transmission performance can be obtained. Actually, a passive device achieving mode order conversion is presented in the current work. In order to implement one-way propagation with the proposed structure, additional physical mechanism should be incorporated into the design. One should note that, Lorentz reciprocity inhibits a linear design to be an optical diode. Therefore, the term 'optical diode' should be reserved for truly non-reciprocal process based approaches. The presence of electro-optic or magneto-optic effects in the design can help breaking the reciprocity. We should notice that there are no such effects considered in the present work.

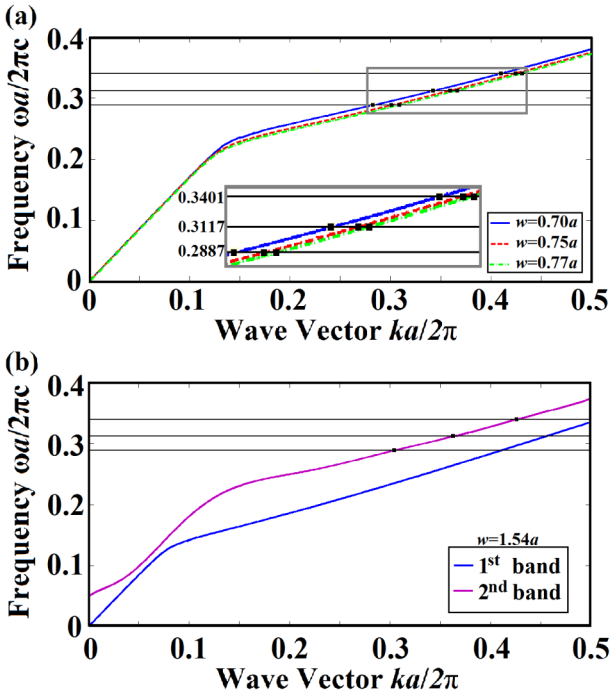


Fig. 6. Dispersion diagrams of the waveguides utilized in the design are computed and plotted for (a) $w = 0.70a$ (b) $w = 0.75a$, (c) $w = 0.77a$ and (d) $w = 1.54a$. Zoom-in part of the operating band dispersion curves is given as an inset. The thickness and dielectric values of the waveguides with $SiO_2$ under-cladding are $t = 0.70a$ and $n = 3.46$. The normalized frequencies of $\omega a/2\pi c = 0.2887$, $\omega a/2\pi c = 0.3117$ and $\omega a/2\pi c = 0.3401$ (lower limit, center and upper limit of the operating bandwidth, respectively) are also indicated in the figure.

#226827 - $15.00 USD Received 13 Nov 2014; revised 12 Jan 2015; accepted 16 Jan 2015; published 3 Feb 2015

## 4. Conclusion

In this 3D study, we numerically demonstrated high contrast ratio mode order converter device with a large operating frequency band. In order to perform conversion process, waveguides with different cross sections are used to obtain π phase shift. In the present study, thickness values of the waveguides are kept constant and only width values are varied. On the other hand, both of these structural parameters can be chosen as variable to enable mode conversion. There is still a potential to reduce $L_c$ by keeping the large bandwidth by these modifications. This study may shed a light on optical isolators with the inclusion of electro-optic or magneto-optic effects. Besides, dispersion compensation and variable attenuation applications can get benefit from the compact and broadband mode order converters.

## Acknowledgments

H. Kurt acknowledges partial support from the Turkish Academy of Sciences.

#226827 - $15.00 USD Received 13 Nov 2014; revised 12 Jan 2015; accepted 16 Jan 2015; published 3 Feb 2015